

Temperature and Pressure Effects on the Resistivity of the Manganese Oxides

Hae-Young Kee and Jongbae Hong

Department of Physics Education, Seoul National University, Seoul 151-742, Korea

Abstract

The temperature and pressure effects on the resistivity of the manganese oxides are studied analytically via the Kondo lattice model with a strong Hund's coupling. We obtain analytically the single-particle density of states on the Bethe lattice in the large connectivity limit using the analytical variant of the dynamic Lanczos method. From the density of states for the doped system, we obtain resistivity and show resistivity drop when temperature crosses the magnetic transition point. We also demonstrate the effect of pressure both below and above the transition temperature.

75.70.Pa, 75.30.Mb, 72.15.Gd

I. INTRODUCTION

Though manganese oxides had been studied extensively during 50's and 60's, [1] the hole-doped manganese oxides $La_{1-x}A_xMnO_3$ ($A = Ca, Ba, Pb, \text{ or } Sr$) have recently driven a considerable attention due to not only the phenomenon of giant magnetoresistance (GMR) [2] but also various interesting physical properties such as doping induced metal-insulator transition, antiferromagnetic-ferromagnetic transition, and the structural phase transition [4]. These phenomena have been partly explained by the double exchange mechanism. [1,5] The ferromagnetic Kondo lattice model (KLM) due to strong Hund's coupling [6] has been proposed to describe the properties of manganese oxides. Recently, a mean field theory, which is valid in infinite dimensions, [7] has been applied to the KLM in the limit of infinite magnitude of local spin. [8] However, the large resistance drop measured in experiment [2] has not been shown successfully. Millis *et al.* have recently argued that the strong electron-phonon coupling is necessary to explain the colossal magnetoresistance [9]. a new experiment [10] shows that there is no primary lattice distortion anomaly at the magnetic transition temperature.

Leaving aside the question how much the polaron physics affects the properties of manganese oxides, we are interested in how well the KLM with a strong Hund's coupling describes the resistivity drop upon variation of temperature [11] and pressure [12–14] in the manganese oxides. We feel that proper calculation of the resistivity in this model is necessary to understand how much the electron-phonon interaction is important for the explanation of the experiments. Even though magnetovolume contraction [15,16] accompanies across the magnetic transition, we do not consider this effect explicitly in this work. We suppose that the effect of pressure is to enhance not only hopping between conduction electrons but also scattering rate. These two effects appear differently in ferromagnetic and paramagnetic states. The purpose of this work is to show quantitatively how much the resistivity drops due to magnetic ordering and pressure via temperature and transfer integral, respectively.

Our work starts from the single-particle density of states (DOS) which has not been

previously obtained through a rigorous calculation for the KLM. We first obtain analytically the DOS of the KLM on the Bethe lattice in the large connectivity. The method we use here, the so called analytic version of the dynamic Lanczos method, has proved useful in describing the optical transport properties of V_2O_3 [17] and the doped cuprates [18]. In a previous work [19], analytical calculation of DOS through this method has given transparent understanding of the metal-insulator transition in the large-dimensional half-filled Hubbard model.

This paper is composed as follows. In Sec. II, we briefly introduce the formalism, and show the single-particle DOS in Sec. III. We present the resistivity depending on temperature and pressure in Sec. IV, and finally give conclusion in Sec. V.

II. FORMALISM

The single-particle DOS, $N_\sigma(\omega)$, is given by [19,22]

$$\begin{aligned} N_\sigma(\omega) &= \frac{1}{\pi N} \lim_{\eta \rightarrow 0^+} \sum_j \text{Re} \int_0^\infty \langle \{c_{j\sigma}(t), c_{j\sigma}^\dagger\} \rangle e^{i\omega t - \eta t} dt \\ &\equiv \frac{1}{\pi} \lim_{\eta \rightarrow 0^+} \text{Re} a_0(z)|_{z=-i\omega+\eta}, \end{aligned} \quad (1)$$

where the angular brackets denote the thermal average and $a_0(z)$, which is the Laplace transform of $\langle \{c_{j\sigma}(t), c_{j\sigma}^\dagger\} \rangle$. One notes that $a_0(z)$ corresponds to the on-site Green function and is the key quantity giving the DOS.

One can observe that $a_0(z)$ is just the projection of $c_{j\sigma}(z)$ onto $c_{j\sigma}$ in a Liouville space defined by the inner product $(A, B) = \langle \{A, B^\dagger\} \rangle$, where A and B are operators of the Liouville space, and B^\dagger is the adjoint of B . This projection can be obtained most easily in the orthogonalized space. Therefore, we first construct an appropriate orthogonal space. We choose the first vector f_0 as $f_0 = c_{j\sigma}$ and the second using the Gram-Schmidt process with a linearly independent vector $iL f_0$ where L is the Liouville operator. The rest orthogonal vectors are obtained via a similar process which may be expressed by the recurrence relation,

$$f_{\nu+1} = iL f_\nu - \alpha_\nu f_\nu + \Delta_\nu f_{\nu-1}, \quad (2)$$

where $f_{-1} \equiv 0$ and $\Delta_\nu = (f_\nu, f_\nu)/(f_{\nu-1}, f_{\nu-1})$ for $\nu \geq 1$. Use of the relation $(iLA, B) = -(A, iLB)$ has been made. Applying Eq. (2) to $f_0(t) = \sum_{\nu=0}^{\infty} a_\nu(t) f_\nu$, the projection $a_0(z)$ is represented by the infinite continued fraction [21–25]

$$a_0(z) = \frac{1}{z - \alpha_0 + \frac{\Delta_1}{z - \alpha_1 + \frac{\Delta_2}{z - \alpha_2 + \ddots}}}, \quad (3)$$

where $\alpha_\nu = (iL f_\nu, f_\nu)/(f_\nu, f_\nu)$.

For a nontrivial system, however, the fractional forms of α_ν and Δ_ν require expansions in performing the Gram-Schmidt process analytically, and allow us an orthogonal set satisfying Eq. (2) exactly only in an asymptotic regime, e.g., strongly or weakly correlated regime. Since α_ν provides with energy standard and can be controlled by chemical potential, α_ν usually has a simple form. What makes things hard is Δ_ν which is the ratio of norms of consecutive bases. Since norm is usually given by a polynomial composed of positive terms of an expansion parameter, the ratio of leading terms gives quite good approximation when the terms of each norm show a similar behavior. This is actually the case we meet in practice. This maybe happens since we get the bases through a simple recurrence relation. We argue that the valid region of the asymptotic dynamics extends to the regime where the expansion is allowed. One can recognize it from the result. One of us and Lee [26,27] have shown the dynamics of electron gas in the asymptotic regimes such as small momentum transfer and large momentum transfer limit. They have shown that the former is good for the regime $k < k_F$ [26], where k and k_F are momentum transfer and Fermi momentum, respectively and the latter agrees well with experiment for the momentum transfer $k \approx 2k_F$ [27].

III. SINGLE-PARTICLE DENSITY OF STATE

We now apply this formalism to the KLM which is written as

$$H = - \sum_{\langle i,j \rangle, \sigma} t_{ij} (c_{i,\sigma}^\dagger c_{j,\sigma} + h.c.) - J \sum_i \mathbf{S}_i \cdot \boldsymbol{\sigma}_i, \quad (4)$$

where angular bracket means nearest neighbor. The first term represents hopping processes of the itinerant electrons in e_g orbital and the second represents ferromagnetic Kondo coupling between localized spin ($S = 3/2$) and itinerant electron spin on Mn^{3+} ion coming from t_{2g} and e_g orbitals, respectively. The electron spin σ_i can be represented in terms of fermion operators. Therefore we have the following Hamiltonian.

$$H = - \sum_{\langle i,j \rangle, \sigma} t_{ij} (c_{i,\sigma}^\dagger c_{j,\sigma} + h.c.) - \frac{J}{2} \sum_i [S_i^- c_{i\uparrow}^\dagger c_{i\downarrow} + S_i^+ c_{i\downarrow}^\dagger c_{i\uparrow} + S_i^z (c_{i\uparrow}^\dagger c_{i\uparrow} - c_{i\downarrow}^\dagger c_{i\downarrow})] \quad (5)$$

where $\mathbf{S} = (S^x, S^y, S^z)$ is a classical spin.

The key part of this work is to construct the orthogonal bases f_ν 's along with α_ν and Δ_ν . Using the recurrence relation (2) with $f_0 = c_{j\uparrow}$ and considering $J \gg t_{ij}$ for expansion, we obtain the orthogonal bases by taking the leading terms as follows:

$$\begin{aligned} f_{4\nu} &= J^{2\nu} \overbrace{\sum'_j \cdots \sum'_q}^{2\nu} \overbrace{t_{kj} \cdots t_{pq}}^{2\nu} \overbrace{\mathbf{T}_k \cdots \mathbf{T}_p}^{2\nu} c_{q\uparrow} \\ f_{4\nu+1} &= i \frac{J^{2\nu+1}}{2} \overbrace{\sum'_j \cdots \sum'_q}^{2\nu} \overbrace{t_{kj} \cdots t_{pq}}^{2\nu} \overbrace{\mathbf{T}_k \cdots \mathbf{T}_p}^{2\nu} (\Delta S_q^z c_{q\uparrow} + S_q^- c_{q\downarrow}) \\ f_{4\nu+2} &= -J^{2\nu+1} \overbrace{\sum'_j \cdots \sum'_r}^{2\nu+1} \overbrace{t_{kj} \cdots t_{qr}}^{2\nu+1} \overbrace{\mathbf{T}_k \cdots \mathbf{T}_p}^{2\nu} [(S_q^z + S_r^z) c_{r\uparrow} + (S_q^- + S_r^-) c_{r\downarrow}] \\ f_{4\nu+3} &= -i \frac{J^{2\nu+2}}{2} \overbrace{\sum'_j \cdots \sum'_r}^{2\nu+1} \overbrace{t_{kj} \cdots t_{qr}}^{2\nu+1} \overbrace{\mathbf{T}_k \cdots \mathbf{T}_p}^{2\nu} \\ &\quad \times [(S_q^z + S_r^z) \Delta S_r^z c_{r\uparrow} + (S_q^- + S_r^-) S_r^+ c_{r\uparrow} + (S_q^z S_r^z - S_q^- S_r^z) c_{r\downarrow} \\ &\quad - (S_q^- + S_r^-) \langle S^z \rangle c_{r\downarrow}] \end{aligned} \quad (6)$$

where $\nu \geq 0$, $\Delta S^z = S^z - \langle S^z \rangle$, $\langle S_k^z \rangle = \langle S_j^z \rangle \equiv \langle S^z \rangle$, and $\mathbf{T}_k = \mathbf{S}_k + \mathbf{S}_j$. We consider only nearest neighbor hopping so that j is the nearest neighbor of k , l is the nearest neighbor of j , and the prime in summation means $k \neq j \neq \cdots \neq r$. The inner operation of $\{\mathbf{T}_k\}$ product is defined as the scalar product only with itself. This operation is valid for classical spins. We obtain the inner products as follows

$$\begin{aligned} (f_1, f_1) &= \langle \frac{J^2}{4} [(\Delta S_k^z)^2 + S_k^- S_k^+] \rangle \\ &= \frac{J^2}{4} (\langle \mathbf{S}_k^2 \rangle - \langle \mathbf{S}_k \rangle^2) \end{aligned}$$

$$\begin{aligned}
(f_2, f_2) &= \langle J^2 \Sigma'_j t_{kj}^2 [(S_k^z + S_j^z)^2 + (S_k^- + S_j^-)(S_k^\dagger + S_j^\dagger)] \rangle \\
&= J^2 \Sigma'_j t_{kj}^2 \langle (\mathbf{S}_k + \mathbf{S}_j)^2 \rangle \\
&= J^2 \Sigma'_j t_{kj}^2 \langle \mathbf{T}_k^2 \rangle \\
(f_3, f_3) &= \frac{J^4}{4} \Sigma'_j t_{kj}^2 \langle \mathbf{T}_k^2 \rangle (\langle \mathbf{S}_j^2 \rangle - \langle \mathbf{S}_j \rangle^2) \\
(f_4, f_4) &= J^4 \Sigma'_j \Sigma'_l t_{kj}^2 t_{jl}^2 \langle \mathbf{T}_k^2 \mathbf{T}_j^2 \rangle \\
&\vdots
\end{aligned} \tag{7}$$

These bases (6) satisfy the orthogonal condition as follow.

$$\begin{aligned}
(f_{4\nu}, f_{4\nu+1}) &= \langle \frac{J^{4\nu+1}}{2} \overbrace{\Sigma'_j \cdots \Sigma'_q}^{2\nu} \overbrace{t_{kj}^2 \cdots t_{pq}^2}^{2\nu} \overbrace{\mathbf{T}_k^2 \cdots \mathbf{T}_p^2}^{2\nu} [(S_q^z - \langle S^z \rangle) \{c_{q\uparrow}, c_{q\uparrow}^\dagger\} + S_q^- \{c_{q\downarrow}, c_{q\uparrow}^\dagger\}] \rangle \\
&= \frac{J^{4\nu+1}}{2} \overbrace{\Sigma'_j \cdots \Sigma'_q}^{2\nu} \overbrace{t_{kj}^2 \cdots t_{pq}^2}^{2\nu} \overbrace{\langle \mathbf{T}_k^2 \rangle \cdots \langle \mathbf{T}_p^2 \rangle}^{2\nu} \langle (S_q^z - \langle S^z \rangle) \rangle = 0
\end{aligned} \tag{8}$$

and so on. We take the approximation neglecting the spatial correlations between the localized spins of Mn^{3+} , that is, $\langle \mathbf{S}_k \cdot \mathbf{S}_j \rangle = \langle \mathbf{S}_k \rangle \cdot \langle \mathbf{S}_j \rangle \equiv \langle \mathbf{S} \rangle^2$ for $k \neq j$. where $\langle \mathbf{S} \rangle$ is independent of sites. Therefore $\langle \mathbf{T}^2 \rangle = 2\langle \mathbf{S}^2 \rangle + 2\langle \mathbf{S} \rangle^2$. Note that this mean field approximation (MFA) is valid in the limit of large connectivity. Within this approximation, one obtains α_ν and Δ_ν as follows:

$$\begin{aligned}
\alpha_{2\nu} &= i \frac{J}{2} \langle \mathbf{S} \rangle \equiv i\alpha, \\
\alpha_{2\nu+1} &= -i \frac{J}{2} \langle \mathbf{S} \rangle \equiv -i\alpha, \\
\Delta_{2\nu+1} &= \frac{J^2}{4} (\langle \mathbf{S}^2 \rangle - \langle \mathbf{S} \rangle^2) \equiv \Delta_o, \\
\Delta_{2\nu+2} &= 4t_*^2 \frac{(\langle \mathbf{S}^2 \rangle + \langle \mathbf{S} \rangle^2)}{(\langle \mathbf{S}^2 \rangle - \langle \mathbf{S} \rangle^2)} \equiv \Delta_e,
\end{aligned} \tag{9}$$

for $\nu \geq 0$, where $t_* = \frac{t}{\sqrt{2q}}$ and q is the coordination number which is taken to be very large.

Now the DOS of the up-spin conduction electron at site j is given by Eqs. (1), (3), and (9), i.e.,

$$N_\uparrow(\omega) = \frac{1}{\pi} \frac{\sqrt{4\Delta_e(\omega^2 - \alpha^2) - (\Delta_o - \Delta_e - (\omega^2 - \alpha^2))^2}}{2|\omega - \alpha|\Delta_e} \tag{10}$$

This DOS shows two separated bands of width $W = \sqrt{\alpha^2 + (\sqrt{\Delta_o} + \sqrt{\Delta_e})^2} - \sqrt{\alpha^2 + (\sqrt{\Delta_o} - \sqrt{\Delta_e})^2}$, which is $4t_*$ when $\langle \mathbf{S} \rangle = 0$, i.e., in paramagnetic state. Eqs. (9) and (10) show that the DOS depends on the magnetic properties of the system through $\langle \mathbf{S} \rangle$ and $\langle \mathbf{S}^2 \rangle$ of the localized spin.

Below the transition temperature T_c , the system is ferromagnetic and the expectation value of $\langle \mathbf{S} \rangle$ can be obtained from the experimental data and $\langle \mathbf{S}^2 \rangle$ is nothing but $S(S+1)$. Above T_c , where the system is paramagnetic, $\langle \mathbf{S} \rangle$ becomes 0 while $\langle \mathbf{S}^2 \rangle$ remains $S(S+1)$.

Fig. 1 shows the DOS for the Hund's coupling strength $J/W = 4$ and a doping concentration $x = 0.3$ using $\langle \mathbf{S} \rangle = 0, 0.4$, and 0.8 with dotted, dashed, and solid lines, respectively. The vertical lines indicate positions of the chemical potential. We only show the lower band since the upper band is nothing but point reflection of lower band about zero frequency, and does not affect resistivity within the range of temperature in which we are interested. The DOS clearly shows the shift of the spectral weight to lower energy side as local spins are ordered. Magnetic ordering enhances up-spin spectral weight and diminishes down-spin spectral weight remarkably. Note that the double exchange model leads us to the rigid band picture and the position of chemical potential is determined only by the amount of filling which results in the change of resistivity upon doping concentration, though our DOS, Eq. (10), does not contain the carrier concentration $\langle n \rangle$. [29] Our DOS satisfies sum rule exactly.

IV. RESISTIVITY

The physical quantity we want to examine in this work is resistivity affected by ordering of magnetic moments and pressure. We show specifically in what follows how magnetic ordering and pressure affect resistivity via obtaining optical conductivity.

Optical conductivity in infinite dimensions is obtained using the following formula [30].

$$\sigma(\omega) = \sigma_0 t_*^2 \int dw' \int d\epsilon A_0(\epsilon) A(\epsilon, \omega') A(\epsilon, \omega' + \omega) \frac{f(\omega') - f(\omega' + \omega)}{\omega} \equiv \sigma_0 I(\omega), \quad (11)$$

where $A_0(\epsilon) = \sqrt{2 - \frac{\epsilon^2}{t_*^2}}/t_*\pi$ for the Bethe lattice, $f(\omega)$ is the Fermi distribution function,

and $\sigma_0 = \frac{\pi e^2 a^2 N}{2\hbar V}$ where a, N, V are lattice constant, number of lattice sites, and volume, respectively.

One can get $A(\epsilon, \omega)$ by calculating the self-energy $\Sigma(\omega)$ using the relation $\Sigma_\sigma(\omega) = \omega - \frac{t_*^2 G_\sigma(\omega)}{2} - \frac{1}{G_\sigma(\omega)}$ applicable to the Bethe lattice [17,31] and $G(\omega) = -ia_0(-i\omega)$. The dc resistivity is obtained by taking the zero-frequency limit for the inverse optical conductivity, i.e.,

$$\rho(T) = \lim_{\omega \rightarrow 0} \frac{1}{\sigma(\omega, T)} = \frac{1}{\sigma_0 I(0, T)}, \quad (12)$$

The unit of conductivity is provided by σ_0 which, in three dimensions, approximately gives Mott's minimum metallic conductivity $\sigma_{Mott} \sim 10^3(\Omega cm)^{-1}$. [8,30] However the absolute value of the resistivity should depend on the microscopic parameters such as lattice constant in σ_0 , so one cannot determine σ_0 precisely. It usually varies of $O(1)$ depending on sample.

Fig. 2 shows temperature dependences of the resistivity for $J/W = 4$ with $x = 0.3$ and magnetization around transition temperature. The magnetization is obtained as $\mathbf{M} = g[\langle \mathbf{S} \rangle + \frac{1}{2}(\langle n_\uparrow \rangle - \langle n_\downarrow \rangle)]$, where g is the g -factor. The temperature dependence of $\langle \mathbf{S} \rangle$ has been conjectured as $\langle \mathbf{S} \rangle = \sqrt{\langle \mathbf{S}^2 \rangle (1 - \frac{T}{T_c})}$ from the mean-field type result, i.e., $\langle \mathbf{S} \rangle \propto \sqrt{1 - \frac{T}{T_c}}$. This magnetic ordering curve shown in Fig. 2 is remarkably similar to the experimental data of magnetization [10]. It shows that the larger magnetic ordering induces the larger resistivity drop. Since it has been known that $La_{1-x}Sr_xMnO_3$ has a bandwidth $W \sim 1eV$ [14], we set $t_* = 0.25eV$ so that the bandwidth $W = 4t_* = 1eV$ in the paramagnetic state, and $J = 4W = 4eV$ which is known as a reasonable value of Hund's coupling. [8] The transition temperature is set $T_c^0 = 0.13t_* = 377K$ to compare with the experiment [10].

We try to understand resistivity drop more physically through the changes of scattering rate and bandwidth versus local spin fluctuation. In Fig. 3, we show the change of scattering rate, $1/\tau_\uparrow$, and bandwidth across T_c to see what governs the resistivity drop. The scattering rate is given by $1/\tau_\uparrow = 2Im\Sigma_\uparrow(\omega = \mu)$, where μ is chemical potential. In Eq. (9) and (10), we see that the DOS has a local spin fluctuation term $\langle (\Delta \mathbf{S})^2 \rangle$. The local spin fluctuation decreases as magnetic ordering increases, which results in broadening of bandwidth and

decreasing of scattering rate of up-spin conduction electron which is parallel to the localized spin. The scattering rate of down-spin conduction electron increases quite rapidly as local spins are ordered. Fig. 3 demonstrates that more spin-disorder scattering occurs in the paramagnetic state, and the spin-disorder strongly affects the scattering rate governing the resistivity.

We show pressure effect by changing the transfer integral t_* for a fixed Hund's coupling strength J . Though the pressure affects both J and bandwidth W , its effect is much larger for W than for J . Therefore we make J fix and W increase as pressure increases. The proportionality $T_c \propto W$ is valid under MFA [6,8], so that T_c is taken at 414K for $W = 1.1\text{eV}$ compared with 377K for $W = 1.0\text{eV}$. Fig. 4 clearly shows that no pressure effect appears in the resistivity above T_c . The origin of this result can be understood as follows. We obtain the effective mass using $m^* = 1 - \frac{\partial \text{Re}\Sigma}{\partial \omega}|_{\omega=\mu}$. The effective mass decreases by increasing t^* , while the scattering rate increases nearly the same amount by increasing t^* , so the effect of change of t^* in the resistivity disappears in the paramagnetic state, if we consider $\rho \propto m^*/\tau$ with assuming constant number of charge carriers. Therefore we have to consider the lattice constant appearing in σ_0 , which will be changed under pressure, to explain the experimental results showing remarkable resistivity drop even above T_c under pressure. The lattice dynamics may play an important role in the paramagnetic regime near T_c . [9]

V. CONCLUSION

We study the temperature and pressure effects on the resistivity of the hole doped manganese oxides by calculating the DOS and optical conductivity for the KLM with strong Hund's coupling using the Lanczos continued fraction formalism along with MFA. These two effects appear in both DOS and resistivity, and the results show that the smaller spin disorder induces the smaller resistivity. Our result also shows that there is no resistivity drop in paramagnetic state, above T_c , under pressure, which has a clear discrepancy with many experimental data [12–14]. It demonstrates that either double exchange model loses

the main physics in the GMR phenomenon or treating the double exchange model within MFA yields too simple physics, which shows that only local spin fluctuation can change resistivity. Above and near T_c , however, the magnetovolume effect may cause further increasing of resistivity due to decreasing of lattice constant in σ_0 of Eq. (12). This effect should be included to improve the resistivity drop just above T_c and to show the pressure effect shown in experiments [12–14], to some extent. Thus present results indicate that lattice distortion may be crucial as far as the resistivity in paramagnet is concerned and polaron may play an important role in this sense.

ACKNOWLEDGMENTS

This work has been supported by SNU-CTP, Basic Science Research Institute Program, Ministry of Education and the Daewoo Foundation. One of authors (H-Y Kee) appreciates Y-B Kim and P. Coleman for useful discussion.

REFERENCES

- [1] G.H. Jonker and J.H. van Santen, *Physica* **16**, 337 (1950); E.O. Wollan and W.C. Koehler, *Phys. Rev.* **100**, 545 (1955); G.H. Jonker, *Physica* **22**, 707 (1956).
- [2] R. M. Kusters *et al.*, *Physica B* **155**, 362 (1989). ; J. Inoue and S. Maekawa, *Phys. Rev. Lett.* **74**, 3407 (1995).
- [3] A. Urushibara *et al.*, *Phys. Rev. B* **51**, 14103 (1995); Y. Tokura *et al.*, *J. Phys. Soc. Jpn*, **63**, 3931 (1994).
- [4] A. Asamitsu, Y. Moritomo, Y. Tomioka, T. Arima, and Y. Tokura, *Nature* **373**, 407 (1995).
- [5] C. Zener, *Phys. Rev.* **82**, 403 (1951); P.W. Anderson and H. Hasegawa, *Phys. Rev.* **100**, 675 (1955); P.G. deGennes, *Phys. Rev.* **100**, 564 (1955).
- [6] K. Kubo and N. Ohata, *J. Phys. Soc. Jpn.* **33**, 21 (1972).
- [7] M.J. Rozenberg, G. Kotliar, and X.Y. Zhang, *Phys. Rev. B* **49**, 10181 (1994).
- [8] N. Furukawa, *J. Phys. Soc. Jpn*, **63**, 3214 (1994); **64**, 2754 (1995).
- [9] A.J. Millis, P.B. Littlewood, and B.I. Shraiman, *Phys. Rev. Lett.* **74**, 5144 (1995).
- [10] M.C. Martin *et al.*, *Phys. Rev. B* to be appeared (1996).
- [11] P. Schiffer *et al.*, *Phys. Rev. Lett.* **75**, 3336 (1995).
- [12] J. J. Neumeier *et al.*, *Phys. Rev. B* **52**, R7006 (1995).
- [13] Z. Arnold *et al.*, *Appl. Phys. Lett.* **67**, 2875 (1995).
- [14] Y. Moritomo *et al.*, *Phys. Rev. B* **51**, 16491 (1995).
- [15] J. M. De Teresa *et al.*, *Solid State Comm.* **96**, 627 (1995).
- [16] M.R.Ibarra *et al.*, *Phys. Rev. Lett.* **75**, 3541 (1995).

- [17] J. Hong and H-Y. Kee, Europhys. Lett. **33**, 453 (1996).
- [18] H-Y. Kee and J. Hong, unpublished.
- [19] J. Hong and H-Y. Kee, Phys. Rev. B **52**, 2415 (1995).
- [20] E. Dagotto, Rev. Mod. Phys. **66**, 763 (1994).
- [21] J. Hong, J. Kor. Phys. Soc. **20**, 174 (1987).
- [22] P. Fulde, *Electron Correlations in Molecules and Solids*, Solid-State Sciences Vol. 100 (Springer-Verlag, Berlin, 1993).
- [23] H. Mori, Prog. Theor. Phys. **34**, 399 (1965).
- [24] R. Zwanzig, in *Lectures in Theoretical Physics* **3**, 106 (1961).
- [25] M. H. Lee, Phys. Rev. B **26**, 2547 (1982); Phys. Rev. Lett. **49**, 1072 (1982); J. Math. Phys. **24**, 2512 (1983).
- [26] M. H. Lee and J. Hong, Phys. Rev. Lett. **48**, 634 (1982).
- [27] J. Hong and M. H. Lee, Phys. Rev. Lett. **70**, 1972 (1993).
- [28] H. E. Stanley, *Introduction to Phase Transition and Critical Phenomena*, (Clarendon Press, Oxford, 1971).
- [29] The filling factor dependence in the DOS appears explicitly when the on-site Coulomb repulsion is included in the Hamiltonian.
- [30] Th. Pruschke, D. L. Cox, and M. Jarrell, Phys. Rev. B **47**, 3553 (1993).
- [31] A. Georges and W. Krauth, Phys. Rev. B **48**, 7167 (1993).

FIGURES

FIG. 1. DOS when $J/W = 4$ for paramagnetic state (a) with dotted line and ferromagnetic state (b) with dashed line and (c) with solid line. We use $\langle \mathbf{S} \rangle = 0.4$ (b) and 0.8 (c). The vertical lines indicate the position of the chemical potential for $x = 0.3$.

FIG. 2. Resistivity and magnetization for $J/W = 4$ and $x = 0.3$ are shown around the transition temperature. Magnetization has been obtained as $g[\langle \mathbf{S} \rangle + \frac{1}{2}(\langle n_{\uparrow} \rangle - \langle n_{\downarrow} \rangle)]$, where g is the g -factor.

FIG. 3. Resistivity (a), bandwidth (b) and scattering rate (c) in units of $10^{-3}\Omega \text{ cm}$, $2t^*$, and $\frac{1}{6} \text{ sec.}^{-1}$ respectively v.s. local spin fluctuation are drawn.

FIG. 4. Resistivities for $W = 1.0eV$ (solid line) and $1.1eV$ (dashed line) with $J = 4eV$, $x = 0.3$ are shown around the transition temperature, where T_c^0 denotes the transition temperature for $W = 1.0eV$

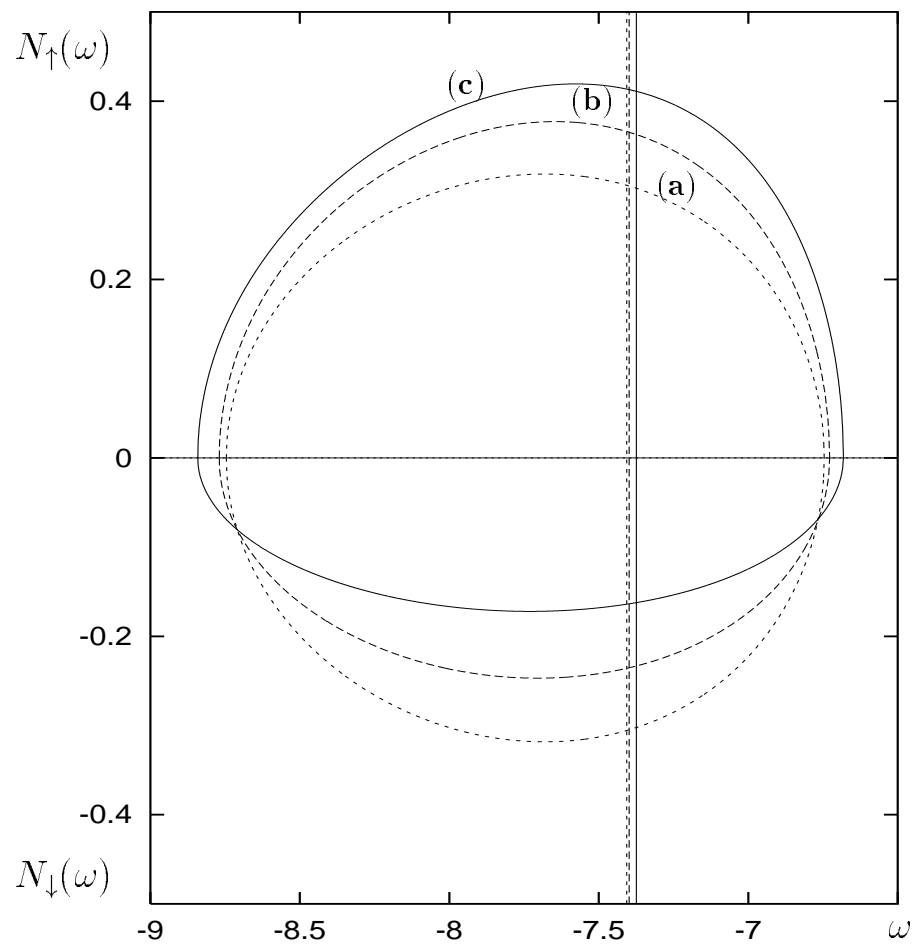


Fig.1

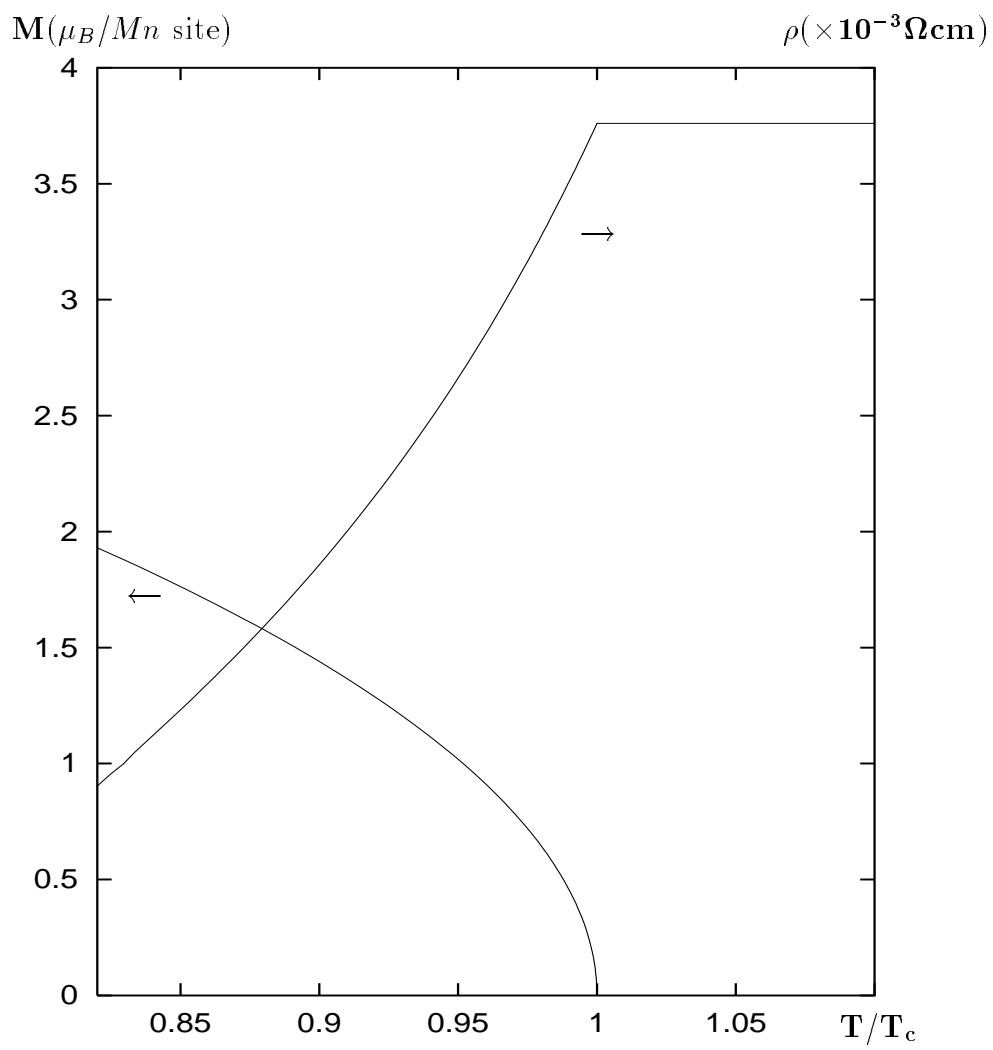


Fig.2

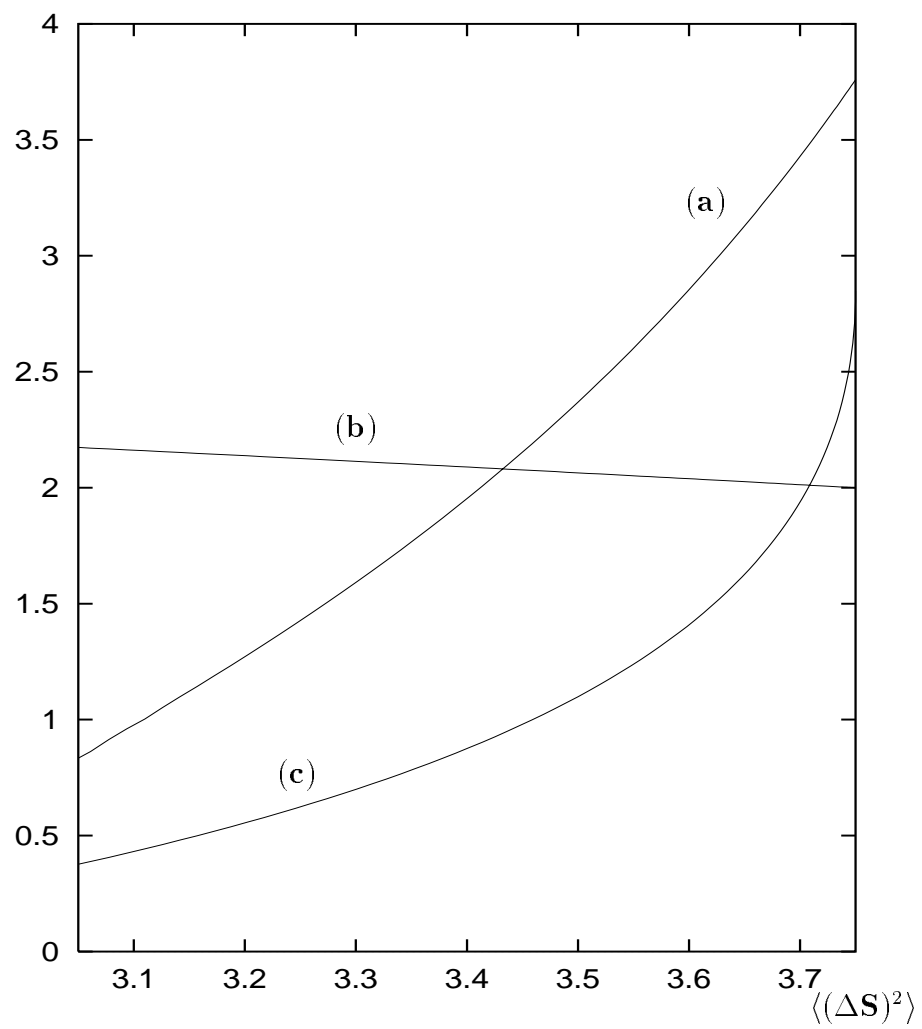


Fig.3

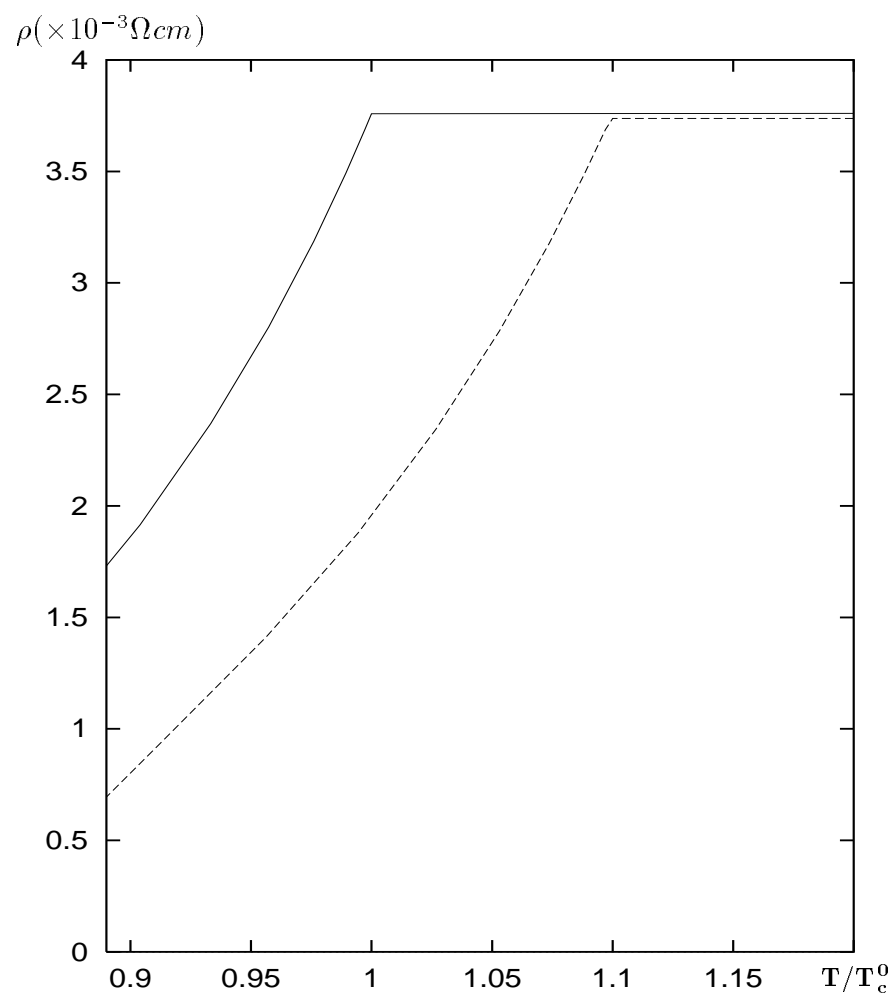


Fig.4